Emission from C-, N- and O-Impurity Ions in Linear Pinch He Plasma in Vaccum Ultraviolet λ500 to 1,500A Region

By

Hidetoshi SUEMITSU*, Yoshio MATSUURA*, Fumio NAKO*
and Kuniya FUKUDA*

(Received June 30, 1976)

Abstract

The He plasma containing C-and O-impurity ions or N-impurity ions, whose electron density and temperature ranged from 5×10^{17} to $3\times10^{18}\,cm^{-3}$ and from 4 to 5 eV, respectively, was produced from He-CO_2 (0.1 mole%) or He-N_2 (0.1 mole%) mixed gas, respectively, in a linear pinch tube, and the observed emission lines in λ500 to 1,500A region were assigned and classified; the lines due to the outer $2s$-shell electron excitation and those due to the valence $2p$-electron excitation for OII-ions, NII-and OIII-ions and CII-, NIII-and OIV-ions, which are specified by the ground state configurations $2s^22p^m$ with $m=3$, 2 and 1, respectively, and the lines from the singly and doubly excited levels for CIII-, NIV-and OV-ions, which have the ground state configuration $2s^2$. The relative intensity, the pressure dependence of intensity and the temporal behavior were observed on the spectral lines of both the outer $2s$ and the valence $2p$ excitations. A possibility is suggested that the charge exchanges between He^+ and impurity atoms or ions take place due to the rapid contraction of the plasma. For CIII- NIV-and OV-ions, it is seen that the lines from the doubly excited level $2p^2(^3P)$ to the metastable levels $2s2p(^3P^o)$ show a remarkable afterglow after the pinch of the plasma.

1. Introduction

Since the middle of the 1950's, the radiation in the visible to ultraviolet region as well as the contraction mechanisms of the linear pinch plasma have been extensively studied by many research workers as described in our previous papers[1,2]. Furthermore, since 1967 the laser radiation from the linear pinch plasma has been investigated by several workers as related in the previous paper,[3] which deals with the ultraviolet laser oscillations from multiply ionized ions in the plasma. Recently, the linear pinch discharge has been applied to the study of the plasma polarization shift by observing the HeII resonance series in the vacuum ultraviolet (VUV) region.[4] However, there are a very few works concerned with the VUV radiation from the linear pinch plasma. The VUV emission from linear pinch Ar plasma

* Department of Engineering Science

was first measured by Blackwell et al.[5] in 1966. Since then no work had been carried out until the detailed observations of the VUV radiation from linear pinch rare gas plasmas by the present authors.[6]

It is, in general, very difficult for us to have an insight into the atomic processes in pinch plasma. The authors analyzed the electromagnetic contraction of plasma at a low pressure in a linear pinch tube.[2] On the basis of this analysis, one of the authors found two types of ionization processes of the plasma from the observation of the ultraviolet laser excitations,[3] namely the very rapid ionization by runaway electrons and the slow successive ionization of atoms by thermal electrons during the plasma compression.

The present experiment was conducted with the aim to elucidate the atomic processes govering the ionization of impurities in the plasma. The He plasmas containing C-, N- or O-ions were produced in a linear pinch tube, and the emission lines of these ions were observed in the λ500 to 1,500A VUV region. In the following section the experimental procedure is described, and in §3, the observed spectral lines are assigned and classified in some groups. In the last section, the characteristic behaviors of the lines in these groups are discussed in connection with the atomic processes in the plasma.

2. Experiment

The linear pinch tube and its operating conditions for the present VUV emission studies were the same as described in our previous paper.[6] The pinch tube was 50 mm in inner diameter and the distance between the electrodes was 120 mm. The tube was operated with C=2 μF and V=15 or 20 kV, and the underdamped discharge current I with the period of about 6 μs had the maximum value of I_{max}=35 kA at the first quarter cycle. These values of the experimental parameters determine the initial gas pressure p_{0M} for the maximum pinch of rare gas plasma, i.e., the pressure giving rise to the maximum density of heavy particles at the pinch time of the plasma.[2] The value of p_{0M} is 0.4 or 0.7 Torr for He pinch discharges with V=15 or 20 kV, respectively.[6]

The experimental set-up is shown in Fig. 2 of our previous paper.[6] The He gas of five nine purity, mixed with CO_2 or N_2 gas of 0.1 mole%, was flowen through the pinch tube from the mixing tank to the differential pumping between the tube and the spectrograph. The initial pressure p_0 in the tube was measured by a Pirani gauge at the inlet to the tube, and it varied from 2.0 to 0.2 Torr. The VUV radiation from the pinch plasma formed along the axis of the tube was observed through a hole of 2 mm diameter in the center of boron nitride cylinder

inside the negative electrode (see Fig. 1 and 2 of ref. 6).

The pinch tube operated with V=20 kV at p_{0M}=0.7 Torr gives an electron density n_e of about 3×10^{18} cm^{-3} and a temperature T_e of about 5 eV at the maximum pinch of pure He, as shown in our calculation and experiment.[2,6]. Furthermore, as the pressure p_0 is decreased from 2.0 to 0.2 Torr through p_{0M}, n_e increases from about 5×10^{17} cm^{-3} to the maximum value at p_{0M} and then decreases back to about 5×10^{17} cm^{-3}. Meanwhile T_e rises up from about 4 eV to 5 eV at p_{0M} and remains almost constant at a lower pressure.[2] Such a behavior of the plasma parameters, n_e and T_e, around the maximum pinch are seen in other experiments.[7,8] On the otherhand, the pinch time τ, i.e., the time until the pinch is formed after the breakdown of discharge, changes only a little, i.e., τ=2 to 1.7~8 μs ($\tau\simeq$1/4 cycle at p_{0M}) between 2.0 and 0.7 Torr. However, it becomes rapidly shorter as p_0 is decreased below p_{0M}, i.e., $\tau<1$ μs at p_0=0.2 Torr. The mixing of a small amount of CO_2 or N_2 is considered to little affect the above behaviors of the plasma parameters as well as the pinch time of the plasma.

For the phorographic and photoelectric observations of VUV emission from C-, N- and O-impurity ions in the He plasma in the λ500 to 1,500A region, there was used a Seya-Namioka spectrograph, Shimazu SGV-50, with a Pt coated grating of radius of curvature 500 mm, 1,200 line per mm and 700A blaze, in which a camera and a photomultiplier attachment were convertible. The reciprocal linear dispersion was 16.6A/mm near λ500A. A photomultiplier tube HTV-1P21 with sodium salicylate phosphor was used for photoelectric detection, and SWR films were used for a photographic record of the spectra. In the latter case, the number of the discharges was controlled by manually triggering the air-gap switch to adjust the exposure on the films.

3. Results of Experiment

In the initial pressure range from 2.0 to 0.2 Torr the spectrum of pure He pinch plasma contains only a small number of very weak spectral lines of impurities such as N-and O-ions, except some weak HeI lines in the λ500 to 1,500A region, although it gives strong line series and continuum of HeII in the λ300 to 150A region.[6] Therefore, the addition of a small amount of CO_2 or N_2 in the host He plasma is expected to give information of the emission from C-, N-and O-impurity ions in the plasma. As the initial pressure is decreased to 0.1 Torr or less, the pure He plasma becomes more turbulent because of very rapid contraction, and emits stronger spectral lines of N-and O-impurity ions. This fact makes it impossible to discriminate the emission of added impurity N-and O-ions.

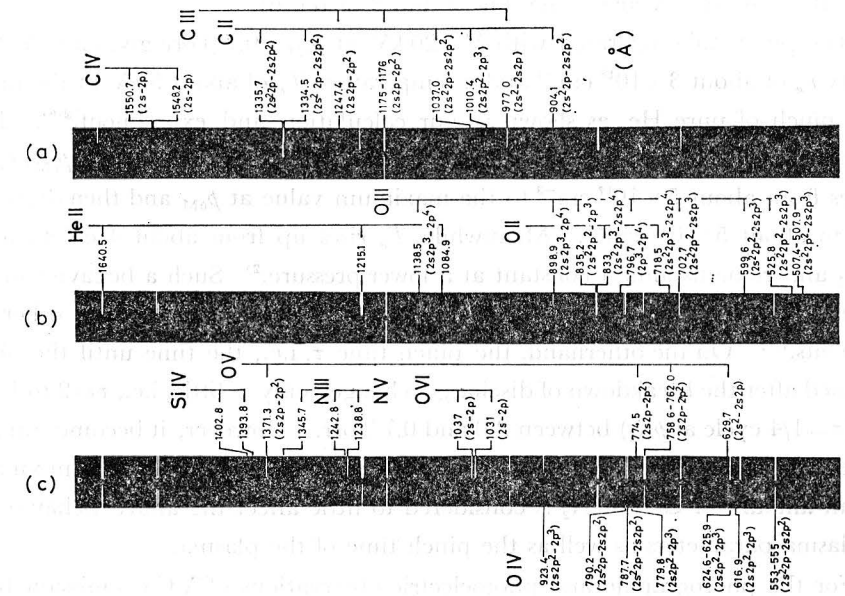

Fig. 1. The spectra of He-CO_2 (0.1 mole %) mixed gas photographed with Seya-Namioka spectrograph. (a) 1.0 Torr, (b) 0.5 Torr and (c) 0.2 Torr. The upper and lower spectra on each photograph correspond to the discharges with 20 and 15 kV, respectively.

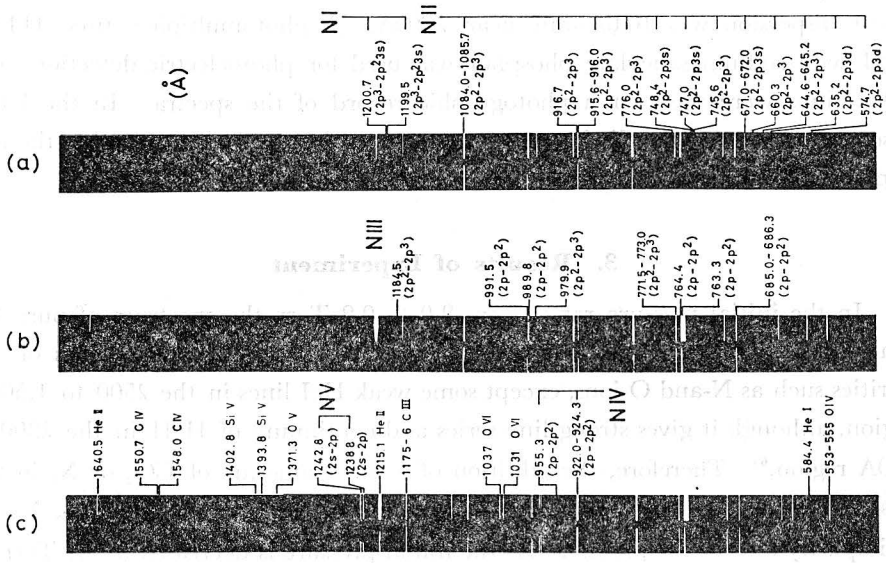

Fig. 2. The spectra of He-N_2 (0.1 mole %) mixed gas photographed with Seya-Namioka spectrograph. (a) 1.0 Torr, (b) 0.5 Torr and (c) 0.2 Torr. The upper and lower spectra on each photograph correspond to the discharges with 20 and 15 kV, respectively.

Figure 1 shows the spectra of C-and O-impurity ion emissions in the He plasma obtained from He-CO_2 (0.1 mole%) gas. Fig. 2 shows the spectra of N-impurity ion emission in the He plasma obtained from He-N_2 (0.1 mole%) gas. In each figure, (a), (b) and (c) correspond to p_0=1.0, 0.5 and 0.2 Torr, respectively, and they include the two spectra, the upper and lower ones, taken for the discharges with V=20 and 15 kV, respectively. In these spectra it is seen that C-, N-and O-spectral lines belonging to the species of a higher ionization stage appear at a lower initial pressure p_0 and also at a higher discharge voltage V.

All observed spectral lines belong to CII and III, NII to IV and OII to V, and are classified according to m=3 to 0 in their ground state electron configuration $2s^22p^m$ as follows,

$$\text{OII: } 2s^22p^3(^4S^\circ_{3/2}) \quad \text{for } m=3, \tag{1}$$

$$\text{NII and OIII: } 2s^22p^2(^3P_0) \quad \text{for } m=2, \tag{2}$$

$$\text{CII, NIII and OIV: } 2s^22p(^2P^\circ) \quad \text{for } m=1, \tag{3}$$

$$\text{CIII, NIV and OV: } 2s^2(^1S_0) \quad \text{for } m=0. \tag{4}$$

Table I (a) VUV Transitions of NII and OIII.

	NII (I.P. 29.59 eV)	OIII (I.P. 54.89 eV)
Outer 2*s*-shell Excitation		
$2s^22p^2(^3P) \leftarrow 2s2p^3(^3D^\circ)$	*1085.1 (1.7–1)	*834.50(1.2–1)
$\leftarrow (^3P^\circ)$	*916.34(2.2–1)	*703.36(1.8–1)
$\leftarrow (^3S^\circ)$	*644.99(2.3–1)	*507.93(1.9–1)
$(^1D) \leftarrow (^1D^\circ)$	*775.96(4.5–1)	*599.60(3.7–1)
$\leftarrow (^1P^\circ)$	*660.28(3.0–1)	*525.79(2.5–1)
$(^1S) \leftarrow (^1P^\circ)$	*745.84(4.0–1)	*597.82(3.5–1)
$2s2p^3(^1P^\circ) \leftarrow 2p^4(^1D)$		1138.5
$(^1D^\circ) \leftarrow (^1D)$		*898.9
Outer 2*p* Excitation		
$2p^2\ (^3P) \leftarrow 2p(^2P^\circ)3d(^3P^\circ)$	*671.48(8.9–2)	374.12(8.1–2)
$(^1D) \leftarrow (^1P^\circ)$	*746.98(1.0–1)	395.56(9.6–2)
$(^1S) \leftarrow (^1P^\circ)$		434.98(1.1–1)
$2p^2\ (^3P) \leftarrow 2p(^3P^\circ)3d(^3D^\circ)$	533.67(2.6–1)	305.72(4.4–1)
$(^3P) \leftarrow (^3P^\circ)$	529.68(8.2–2)	303.66(1.4–1)
$(^1D) \leftarrow (^1D^\circ)$	582.15(6.4–2)	328.45(9.9–2)
$\leftarrow (^1F^\circ)$	*574.65(2.4–1)	320.98(4.1–1)
$\leftarrow (^1P^\circ)$	572.07(2.9–3)	302.34(5.2–3)
$(^1S) \leftarrow (^1P^\circ)$	635.18(3.2–1)	345.31(5.3–1)

The number in parentheses indicates the oscillator strength, for example, (1.7–1) means 1.7×10^{-1}.

* The observed spectral lines.

Table I (b) VUV Transitions of CII, NIIIand OIV

	CII (I.P. 24.38 eV)	NIII (I.P. 29.59 eV)	OIV (I.P. 77.39 eV)
Outer $2s$-shell Excitation			
$2s^22p(^2P^o) \leftarrow 2s2p^2(^2D)$	*133.53(2.7–1)	*991.0(1.8–1)	*789.4(1.5–1)
$\leftarrow (^2S)$	*1036.8(5.9–2)	*764.0(1.1–1)	*607.4(1.0–1)
$\leftarrow (^2P)$	*904.1(5.2–1)	*685.7(4.5–1)	*554.4(3.8–1)
$2s2p^2(^4P) \leftarrow 2p^3 (^4S^o)$	*1010.2(1.6–1)	*772.1(1.7–1)	*625.4(1.4–1)
$(^2D) \leftarrow (^2D^o)$	*1323.9(2.3–1)	*979.9(2.0–1)	
$\leftarrow (^2P^o)$	*1066.0(8.3–2)	*772.9(8.6–2)	*616.9
$(^2S) \leftarrow (^2P^o)$		*1006.0(2.7–1)	
$(^2P) \leftarrow (^2D^o)$	2511.0(1.5–1)	*1750.4(2.0–1)	*779.8
$\leftarrow (^2P^o)$		*1184.0(1.8–1)	*923.4
Outer $2p$ Excitation			
$2p(^2P^o) \leftarrow (^1S)3s(^2S)$	*858.4(4.6–1)	452.1(4.6–1)	279.8(5.0–1)
$\leftarrow (^1S)3d(^2D)$	*687.3(2.6–1)	374.4(3.9–1)	238.5(5.0–1)

The number in parentheses indicates the osicllator strength, for example, (2.7–1) means 2.7×10^{-1}.
* The observed spectral lines.

Table I (c) VUV Transitions of CIII, NIV and OV

	CIII (I.P. 47.86 eV)	NIV (I.P. 77.45 eV)	OV (I.P. 113.83 eV)
Two-Electron Esxcitation			
$2s2p(^3P^o) \leftarrow 2p^2(^3P)$	*1175.7(2.6–1)	*923.2(2.1–1)	*760.4(1.8–1)
$(^1P^o) \leftarrow (^1D)$	2296.9(4.7–1)	1718.5(3.8–1)	1371.3(3.2–1)
$(^1P^o) \leftarrow (^1S)$	*1247.4(9.0–2)	*955.3(7.4–2)	*774.5(6.2–2)
One-Electron Excitation			
$2s^2 (^1S) \leftarrow 2s(^2S)2p(^1P^o)$	*977.0(8.1–1)	*765.1(6.4–1)	*629.7(5.3–1)
$\leftarrow 3p(^1P^o)$	386.2(2.6–1)	247.2(5.5–1)	172.2(5.9–1)
$\leftarrow 4p(^1P^o)$	310.2(1.6–2)		
$2s2p(^3P^o) \leftarrow 3s(^3S)$	*538.2(3.1–2)	322.7(5.9–2)	215.2(4.88–2)
$(^1P^o) \leftarrow (^1S)$	690.5(5.3–2)	387.4(4.9–2)	248.5(4.24–2)
$(^3P^o) \leftarrow 3d(^3D)$	459.6(4.2–1)	283.5(6.3–1)	192.9(6.4–1)
$(^1P^o) \leftarrow (^1D)$	*574.3(5.2–1)	335.1(5.3–1)	220.4(5.6–1)
$(^3P^o) \leftarrow 4d(^3D)$	371.7(1.2–1)	225.2(1.2–1)	

The number in parentheses indicates the oscillator atrength, for example, (2.6–1) means 2.6×10^{-1}.
* The observed spectral lines.

In Table I (a), (b) and (c) are listed all VUV transitions of NII-type, CII-type and CIII-type ions together with absorption oscillator strengths, respectively, where the observed transitions are indicated by asterisks.[9,10,11] In Table II are given all VUV transitions of OII ions together with the relative intensity of observed spectral lines. Furthermore, Figs. 3, 4 and 5 also show the energy diagrams of

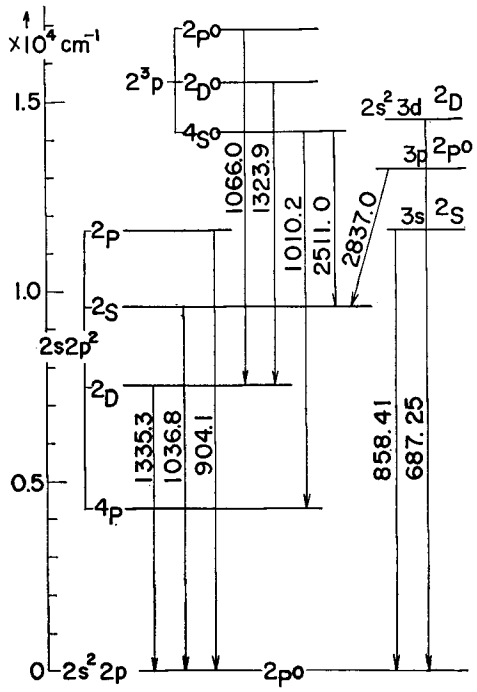

Fig. 3. The energy diagram of CII. Wavelength in A is inidcated for the transitions.

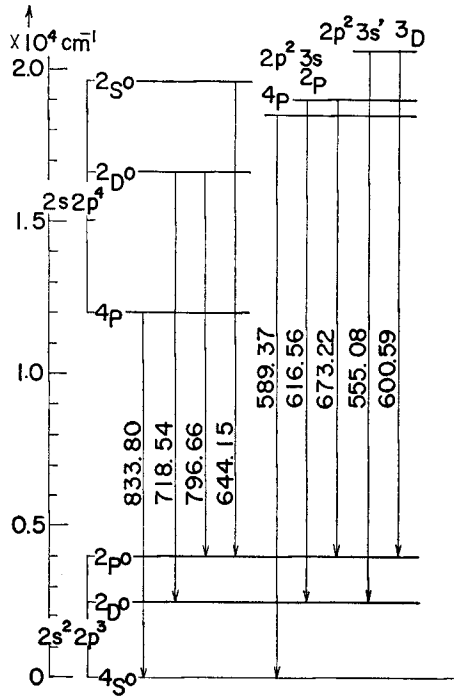

Fig. 5. The energy diagram of OII. Wavelength in A is indicated for the transitions.

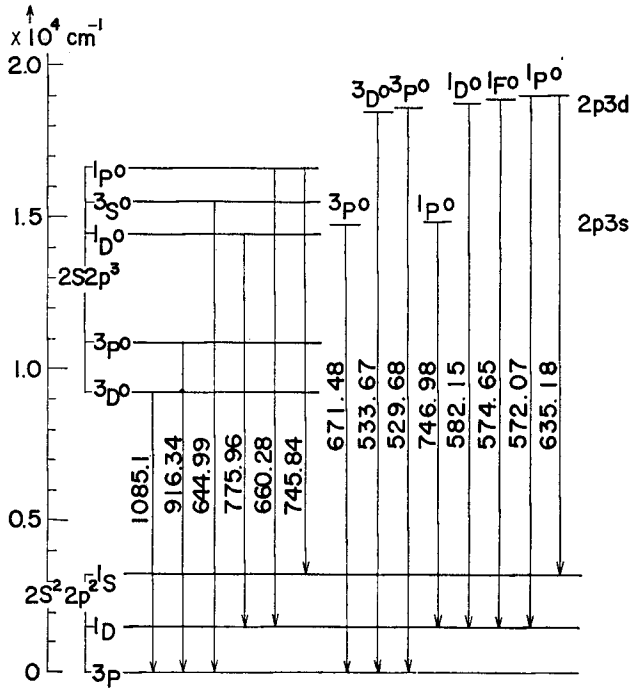

Fig. 4. The energy diagram of NII. Wavelength in A is indicated for the transitions.

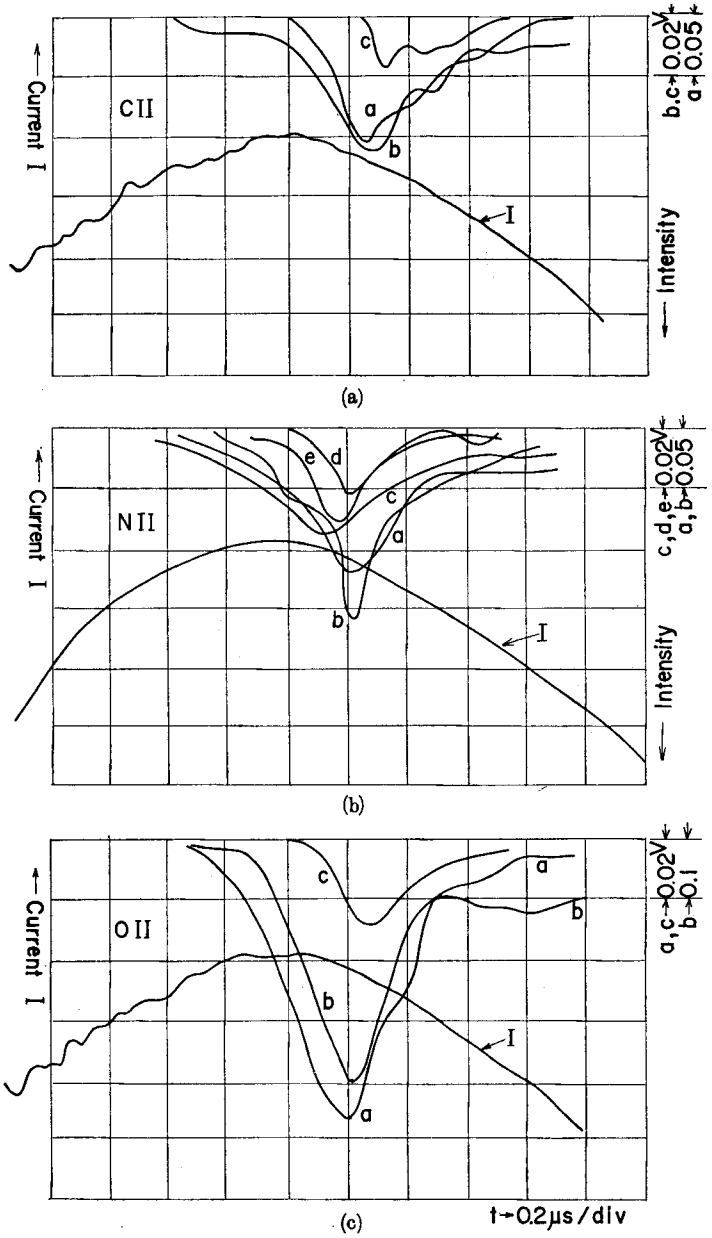

Fig. 6. The temporal behavior of the intensities of CII, NII and OII spectral lines for the discharge with 20 kV at p_0=0.5 Torr, where the upper traces are the line intensities and the lower trace is the discharge current I in each figure.

(a) CII: a. 904.1A $2s^22p(^2P^o) \leftarrow 2s2p^2(^2P)$, b. 858.4A $2s^22p(^2P^o) \leftarrow 2s^23s(^2S)$, c. 687.3A $2s^22p(^2P^o) \leftarrow 2s^23d(^2D)$.

(b) NII: a. 1085.1A $2s^22p^2(^3P) \leftarrow 2s2p^3(^3D^o)$, b. 916.3A $2s^22p^2(^3P) \leftarrow 2s2p^3(^3P^o)$, c. 776.0A $2s^22p^2(^1D) \leftarrow 2s2p^3(^1D^o)$, d. 671.5A $2s^22p^2(^3P) \leftarrow 2p3s(^3P^o)$, e. 574.6A $2s^22p^2(^1D) \leftarrow 2p3d(^1F^o)$.

(c) OII: a. 718.5A $2s^22p^3(^2D^o) \leftarrow 2s2p^4(^2D)$, b. 833.8A $2s^22p^3(^4S^o) \leftarrow 2s2p^4(^4D)$, c. 673.2A $2s^22p^3(^2P^o) \leftarrow 2p^23s(^2P)$.

CII, NII and OII, respectively, where use is made of the tables given by Wiese.[9]

All the VUV spectral lines of the species of the $2s^22p^m$ configuration with $m \neq 0$ are classified into the following two types;

$$2p^{m+2} \rightarrow 2s2p^{m+1} \rightarrow 2s^22p^m \text{ (ground state)}, \quad (5)$$

and

$$2s^22p^{m-1}3s \text{ or } 3d \rightarrow 2s^22p^m \text{ (ground state)}. \quad (6)$$

The former is concerned with the outer $2s$-shell electron excitation, including the two $2s$-electron excitation, and the latter is concerned with the valence $2p$-electron excitation. The transitions of both types, (5) and (6), are seen in the spectra of CII-, NII- and OII-ions. However, only the transitions of type (5) are observed in the spectra of NIII-, OIII- and OIV-ions, where the transitions of type (6) lie below λ500A, the shorter wavelength limit of the Seya-Namioka spectrograph. The transitions from the levels of the two $2s$-electron excitations are observed in the spectra of CII-, NIII-, OIII- and OIV-ions as shown in Table I (a) and (b).

In the spectra of CII-, NII- and OII-ions the spectral lines due to the outer $2s$-shell electron excitation are more strongly observed than the lines due to the valence $2p$-electron exictation, as shown in the oscilloscope traces of the photoelectric signals of the lines in Figs. 6 (a) to (c). In Tables II, III and IV are

Table II VUV transitions of OII.

OII $2s^22p^3(^4S^o_{3/2})$: 35.10 eV

Transitions	λ	A (10^8 sec^{-1})	Intensity PG	Intensity PE	Rel. Pop.
$2s^22p^3(^4S^o)$ *GS*←$2s2p^4(^4P)$	833.8 A	14	*s*	9.0	1
: $(^2D^o)$ ← : (^2D)	718.54	32	*vw*	0.6	0.024
: $(^2P^o)$ ← : (^2D)	796.66_1	4.4	*vw*		
: ← : (^2S)	644.14_8	72	—		
$2s^22p^3(^4S^o)$ *GS*←$2p^2(^3P)3s(^4P)$	539.37	8.6	—		
: $(^2D^o)$ *GS*← : (^4P)	616.56	18	—		
: $(^2P^o)$ ← : (P_2)	673.22	9.2	—	0.3	0.039
$2s^22p^3(^2D^o)$ ←$2p^2(^1D)3s'(^2D)$	555.08	15	—		
: $(^2P^o)$ ← : (^2D)	600.58_5	4.3	—		
$2s^22p^3(\cdots)$ ←$2p^2(^3P)3d$ and $(^1D)3d'$, 12 lines 500–400					

The relative intensity is given for the spectrum of the discharge with V=20 kV and C=2μF at p_0=0.5 Torr.

A : Transition probability.
PG : Intensity on photographic films.
PE : Intensity of photoelectric signals.
s : Strong. *vw* : Very weak.

Table III VUV transitions of NII.

NII $2s^22p^2(^3P_0)$: 29.593 eV

Transitions		λ	A (10^8 sec^{-1})	Intensity PG	Intensity PE	Rel. Pop.
$2s^22p^2(^3P)$	$GS\leftarrow 2s2p^3(^3D^o)$	1085.1 A	5.7	*s*	24	5
	$\leftarrow$: $(^3P^o)$	916.34	18	*s* (17)	17	1
	$\leftarrow$: $(^3S^o)$	644.99	110	*w* (6.2)	10*	0.07
$2s^22p^2(^1D)$	$\leftarrow 2s2p^3(^1D^o)$	775.96	49	*w* (10)	13	0.24
	$\leftarrow$: $(^1P^o)$	660.28	77	*vw*(3.5)	5	0.04
$2s^22p^2(^1S)$	$\leftarrow$: $(^1P^o)$	745.84	16	*w* (6.8)	7**	
$2s^22p^2(^3P)$	$GS\leftarrow 2p(^2P^o)3s(^3P^o)$	671.48	13	*vw*(4.6)	4.4	0.26
	$\leftarrow$: $(^1P^o)$	746.98	20	*w* (6.8)	7**	0.30
$2s^22p^2(^1D)$	$\leftarrow 2p(^2P^o)3d(^1F^o)$	574.65	35	*vw*(3.0)	2.7	0.05
: (^1S)	$\leftarrow$: $(^1P^o)$	635.18	18	*vw*		

The relative intensity is given for the spectrum of the discharge with V=20 kV and C=2 μF at p_0=0.5 Torr.

A : Transition probability.
PG : Intensity on photographic films.
PE : Intensity of photoelectric signals.
s : Strong. *w* : Weak. *vw* : Very weak.

* Superposed on OII-644.14 A line.
** The two lines are not resolved.

Table IV VUV Transitions of CII.

CII $2s^22p(^2P^o)$: 24.367 eV

Transitions		λ	A (10^8 sec^{-1})	Intensity PG	Intensity PE	Rel. Pop.
$2s^22p(^2P^o)$	$GS\leftarrow 2s2p^2(^2D)$	1335.3 A	6.0	*s*		
:	$\leftarrow$: (^2S)	1036.8	11	*s*		
:	$\leftarrow$: (^2P)	904.1	42	*s*	22	1
$2s2p^2(^4P)$	$\leftarrow 2p^3(^4S^o)$	1010.2	32	*s*		
$2s^22p(^2P^o)$	$GS\leftarrow(^1S)3s(^2S)$	858.4	12	*vw*	3	0.453
:	$\leftarrow(^1S)3d(^2D)$	687.2_5	22	*vw*	8	0.528

The relative intensity is given for the spectrum of the discharge with V=20 kV and C=20 μF at p_0=0.5 Torr.

A : Transition probabirity.
PG : Intensity on photographic films.
PE : Intensity of photoelectric signals.
S : Strong. *vw*: Very weak.

listed the observed VUV lines of OII, NII and CII, respectively, together with their relative intensity I_{rel} observed at p_0=0.5 Torr for the discharge with V= 20 kV. The tables also include the Einstein *A*-coefficients and the relative po-

pulation densities n of the upper levels for the transitions concerned, where n is calculated from $I_{rel}=A\,n\,hc\lambda^{-1}$ under the assumption of the optically thin plasma. Here the designations such as s(strong) and w(weak) indicate the line intensity on photographic films in a very qualitative sense (PG). The numbers indicating the relative intensity are determined from the line intensities observed at the pinch time with a photomultiplier, i.e., the peak photoelectric signals of the emission lines (PE). The photoelectric relative intensity, of course, includes the spectral response of the spectrograph.

For the photographic spectra of NII-ion emission lines, the characteristic curve of SWR film was made on some different wavelength regions by adjusting the shot numbers of the pinch discharges to get appropriate exposures. The relative intensity as well as the pressure dependence of intensity were obtained on several lines. The relative intensity determined by this method is also indicated by the numbers in the parentheses in the column PG of Table III, and is in good agreement with the relative intensity determined from the photoelectric signals. This is because of the very strong emission from the pinch plasma at its first quarter cycle. In the table it is clearly seen that the spectral lines due to the outer $2s$-shell electron excitation, especially the lines from $2s2p^3(^3D^o)$ and $(^3P^o)$, are much stronger than those of the valence $2p$-electron excitation.

The photographically determined pressure dependence of the VUV NII-ion lines is shown for the discharge with V=20 kV in the pressure range from 2.0 to

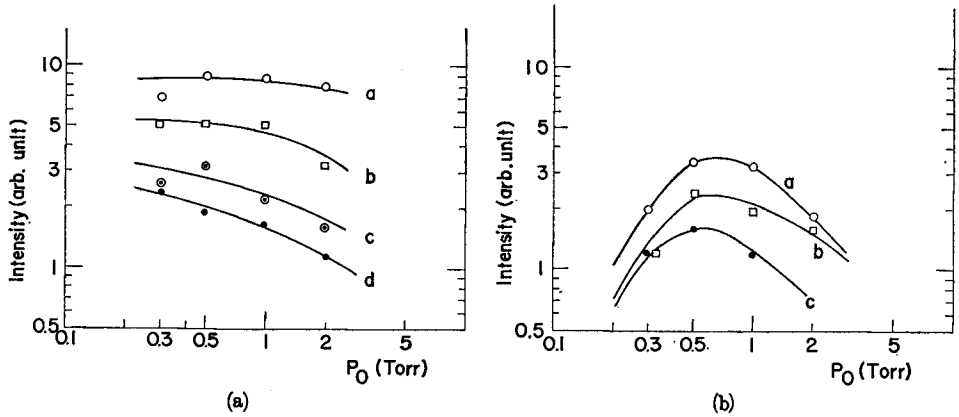

Fig. 7. The pressure dependence of the intensities of the VUV NII lines for the discharge with 20 kV.

(a) the outer $2s$-shell electron excitation:
a. 915.6A $2s^22p^2(^3P)\leftarrow 2s2p^3(^3P^o)$, b. 776.0A $2s^22p^2(^1D)\leftarrow 2s2p^3(^1D^o)$, c. 645.0A (superposed on OII 644.2A) $2s^22p^2(^3P)\leftarrow 2s2p^3(^3S^o)$, d. 660.3A $2s^22p^2(^1D)\leftarrow 2s2p^3(^1P^o)$.

(b) the valence $2p$-electron excitation:
a. 747.0A $2s^22p^2(^1P)\leftarrow 2p(^2P^o)3s(^1P^o)$, b. 671.5A $2s^22p^2(^3P)\leftarrow 2p(^2P^o)3s(^3P^o)$, c. 574.7A $2s^22p^2(^1D)\leftarrow 2p(^2P^o)3d(^1F^o)$.

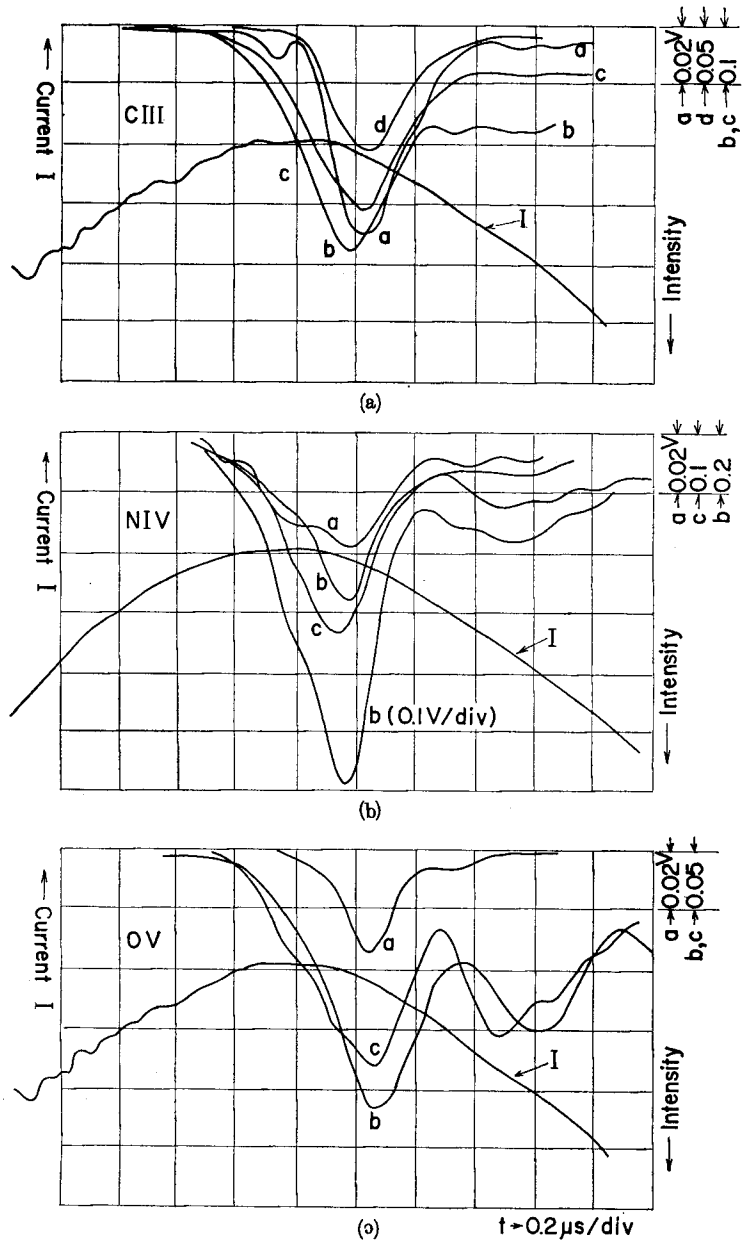

Fig. 8. The temporal behavior of the intensities of the VUV CIII, NIV and OV lines for the discharge with 20 kV at $p_0=0.5$ Torr, where the upper traces are the line intensities and the lower trace is the discharge current I in each figure.

(a) CIII: a. 1247.4A $2s2p(^1P^o) \leftarrow 2p^2(^1S)$, b. 1175.7A $2s2p(^3P^o) \leftarrow 2p^2(^3P)$, c. 977.0A $2s^2(^1S) \leftarrow 2s2p(^1P^o)$. d. 538.2A $2s2p(^3P^o) \leftarrow 2s3s(^3S)$.

(b) NIV: a. 955.3A $2s2p(^1P) \leftarrow 2p^2(^1S)$, b. 923.2A $2s2p(^3P^o) \leftarrow 2p^2(^3P)$, c. 765.1A $2s^2(^1S) \leftarrow 2s2p(^1P^o)$.

(c) OV: a. 774.5A $2s2p(^1P^o) \leftarrow 2p^2(^1S)$, b. 760.4A $2s2p(^3P^o) \leftarrow 2p^2(^3P)$, c. 629.7A $2s^2(^1S) \leftarrow 2s2p(^1P^o)$.

0.2 Torr in Fig. 7 (a) and (b). As the pressure is decreased from p_0=2.0 Torr, the intensity of the lines due to the outer 2*s*-shell electron excitation remains constant or becomes higher as shown in (a). However, the intensity of the lines of the valence 2*p*-electron excitation decreases through the maximum at around p_{0M} as shown in (b).

In the spectra of CIII-type ions (4) with the ground state configuration $2s^2$, there were observed the lines of several types of transitions (see Table I (c)), namely transitions from doubly excited levels,

$$2p^2(^3\mathrm{P}) \rightarrow 2s2p(^3\mathrm{P}^o) \text{ in triplet system,} \quad (7)$$

$$2p^2(^1\mathrm{P}) \rightarrow 2s2p(^1\mathrm{P}^o) \text{ in singlet system,} \quad (8)$$

and transitions from a singly excited state,

$$2s2p,\ 3p,\ \cdots(^1\mathrm{P}) \rightarrow 2s^2(^1\mathrm{S}) \text{ resonance series,} \quad (9)$$

$$2s3s \text{ or } 3d \rightarrow 2s2p \text{ in singlet and triplete systems.} \quad (10)$$

As shown in the photoelectric signals of CIII, NIV- and OV-ion lines in Figs. 8 (a), (b) and (c), respectively, the resonance lines (9) and the doubly excited triplet lines (7) are very intense, while the doubly excited singlet lines (8) are weak. Considering the magnitudes of the Einstein *A*-coefficients of these three-type transitions (approximately 2:2:3 against (7): (8):(9) for all the ions), the population density of the $2p^2(^3\mathrm{P})$ level is very large. Furthermore, the doubly excited triplet lines (7) show an afterglow after the pinch of the plasma. This phenomenon is remarkable, especially for the OV-ion as shown in Fig. 8 (c).

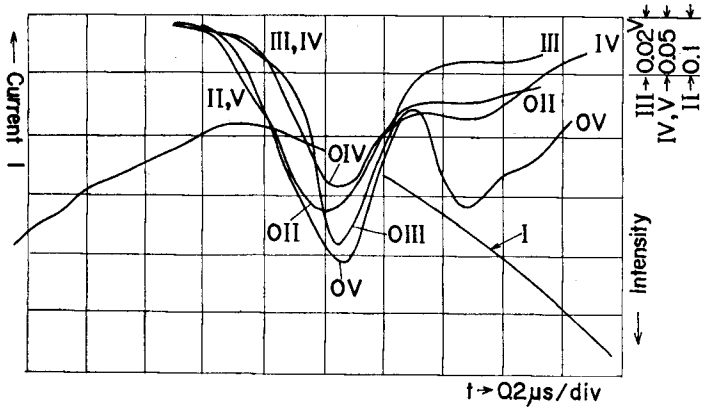

Fig. 9. The temporal behavior of the intensities of OII, OIII, OIV and OV lines for the discharge with 20 kV at p_0=0.5 Torr.
Upper traces: OII 833.8A $2s^22p^3(^4\mathrm{S}^o) \leftarrow 2s2p^4(^4\mathrm{P})$, OIII 599.6A $2s^22p^2(^1\mathrm{D}) \leftarrow 2s2p^3(^1\mathrm{D}^o)$, OIV 607.4A $2s^22p(^2\mathrm{P}^o) \leftarrow 2s2p^2(^2\mathrm{S})$ and OV 629.7A $2s^2(^1\mathrm{S}) \leftarrow 2s2p(^1\mathrm{P}^o)$.
Lower trace: discharge current.

As seen in Figs. 6 (a) to (c) the CII-, NII- and OII-ion lines of both the outer $2s$-shell electron and the valence $2p$-electron excitations show their peaks of emission nearly at the same time, i.e., at the pinch time. The cascading two lines of $2p^{m+2} \rightarrow 2s2p^{m+1} \rightarrow 2s^2 2p^m$ also showed their peaks at the pinch time in the photoelectric observations of CII-, NIII-, OIII- and OIV-ion spectra. A time difference larger than 0.1 μs (the time resolution limit of the measurement) was not observed on the appearance of the peaks of photoelectric signals for all kinds of transitions from (5) to (10). Figure 9 shows the temporal behaviors of the spectral lines of OII- to OV-ions, where all the transitions are concerned with the $2s$-electron excitation. The intensity peaks of these lines almost coincide with the pinch time, and the successive appearance of the impurity ion lines in the order of increasing ionization stage is not seen.

4. Discussions

The VUV emission lines from C-, N- and O-impurity ions embedded in the host He pinch plasma show the following characteristic behaviors.

The spectral lines due to the outer $2s$-shell electron excitation appear more strongly at the pinch time than those of the valence $2p$-electron excitation. The pressure dependence of the intensity for the latter in Fig. 7 (b) is similar to that of the electron density of the host He plasma, which is given in Fig. 5 of ref. 2. The pressure dependence of Fig. 7 (a) for the former is very different and the intensity of the lines rather increases with decreasing gas pressure. This intensity increase seems to be related to the increase of the contraction speed of the plasma with a decrease of the filling gas pressure.

The impurity ion-lines of all kinds of transitions from (5) to (10) show their emission peaks nearly at the pinch time as seen in Figs. 6, 8 and 9, and the successive appearance of ion-lines in the increasing order of the ionization stage is not seen. This fact is not explained from the ionization of impurity ions by thermal electrons with an increasing electron density and temperature during the contraction of the host He plasma.

The intensity of highly ionized impurity ion-lines, especially the lines of the outer $2s$-shell electron excitation, appear much more strongly than expected. For example, the ratio among the peak intensities of the O-ion lines in Fig. 9 can not be obtained from the assumption of LTE on the upper levels of the transitions with a Saha equilibrium among the impurity ions for the optically thin plasma which has the electron density of 3×10^{18} cm^{-3} and temperature of 5 eV.

Immediately after the breakdown of the discharge, a plasma of low ionization is formed in the whole volume of the Z-pinch tube, and then the current sheet

rapidly grows up due to the skin effect with an increasing discharge current. The plasma column inside this current sheet is adiabatically compressed by the magnetic field surrounding the column. The speed of the contracting current sheet is approximately 10^7 cm/s (0.1 a.u.) (from Fig. 1 of ref. 2). Accordingly, the particles pushed by the current sheet collide with the particles in the center part with a kinetic energy of about 1 kV for He or about 4 kV for O atoms or ions.

Combining the above observed behaviors of the impurity ion VUV emissions with this model of contracting plasma, it is plausible that the impurity atoms are ionized and emit a VUV radiation due to the outer $2s$-shell excitation by the charge exchange collision.[12-14] For example,

$$\begin{aligned} \mathrm{He}^+(1s)+\mathrm{X}_Z(2s^2 2p^m) &\rightarrow \mathrm{He}+\mathrm{X}_{Z+1}(2s2p^m) \\ &\rightarrow \mathrm{He}+\mathrm{X}_{Z+1}(2s^2 2p^{m-1})+h\nu \ (\mathrm{VUV}) , \end{aligned}$$

where X_Z stands for impurity atoms with $Z=0$ and for impurity ions with $Z\neq 0$. In order to get more definite proof for the above process further experiment is necessary in the wavelength region shorter than λ500A, where we have many spectral lines due to both the outer $2s$-shell electron and the valence $2p$-electron excitations.

References

1) K. Ishii, H. Suemitsu and K. Fukuda: Japan. J. appl. Phys. 5 (1966) 1235.
2) Y. Hashino, H. Suemitsu and K. Fukuda: Japan. J. appl. Phys. 11 (1972) 710.
3) Y. Hashino, Y. Katsuyama and K. Fukuda: Japan. J. appl. Phys. 13 (1974) 1134.
4) T. Goto and D. D. Burgess: J. Phys. B, Atom. Molec. Phys. 7 (1974) 857.
5) H. Blackwell, G. S. Shipp, M. Ogawa and G. L. Weissler: J. Opt. Soc. Amer. 56 (1966) 665.
6) K. Fukuda, H. Suemitsu and M. Ota: Japan. J. appl. Phys. 13 (1974) 463.
7) H. Zwicker and U. Schumacher: Z. Phys. 183 (1965) 453.
8) D. D. Burgess, A. E. Dangor and J. E. Jenkins: Brit. J. appl. Phys. 18 (1967) 1281.
9) W. L. Wiese, M. W. Smith and B. M. Glennon: Atomic Transition Probabilities (U. S. Government Printing Office, Wshington D. C., 1966) vol. 1.
10) A. H. Zaidel', B. K. Prokof'ev, C. M. Raickii, B. A. Clavnyi and E. Ya. Shreider: Tablitsy Spektral'nykh Linii (Nauka, Moskva, 1969).
11) R. L. Kelly: Vacuum Ultraviolet Emission Lines (UCRL 5612, Univ. Calif. Lawrence Rad. Lab., 1960).
12) U. Fano and W. Lichten: Phys. Rev. Letters, 14 (1965) 627.
13) W. Lichten: Phys. Rev. 164 (1967) 163.
14) M. Barat and W. Lichten: Phys. Rev. A6 (1972) 211.